Right Ventricular Thallium-201 Kinetics in Pulmonary Hypertension: Relation to Right Ventricular Size and Function

Douglas S. Schulman, Jason M. Lazar, Galal Ziady, Donald J. Grandis, Angel R. Flores and Judith E. Orie

Department of Medicine, Section of Cardiology, Medical College of Pennsylvania; and University of Pittsburgh, Pittsburgh, Pennsylvania

Right ventricular ischemia occurs in experimental models of pulmonary hypertension. We analyzed right ventricular size and function and ^{201}Tl uptake to determine if there was a relationship between ^{201}Tl uptake and systolic function in 19 patients with pulmonary artery hypertension who were being evaluated for heart-lung transplantation. All patients had dipyridamole stress ^{201}Tl scintigraphy, radionuclide angiography and echocardiography. In nine patients (Group 1), right ventricular ejection fraction was <30% (mean 22% ± 8%). In 10 patients (Group 2) it was >30% (mean 45% ± 11%). In Group 1, right ventricular ^{201}Tl uptake in the lateral wall after dipyridamole was increased compared to Group 2 (40% ± 7% versus 28% ± 15% counts/pixel, $p < 0.05$) while left ventricular free wall uptake was similar. The ratio of right to left ventricular ^{201}Tl uptake was increased in Group 1 versus Group 2 (0.81% ± 0.30% versus 0.49% ± 0.18%, $p < 0.05$). At 4 hr, right ventricular free wall ^{201}Tl clearance was comparable, 51% ± 13% versus 51% ± 18% in Groups 1 and 2, respectively. No patient had perfusion abnormalities. Right ventricular ejection fraction was inversely related to dipyridamole stress right ventricular ^{201}Tl uptake, $r = -0.49$, $p < 0.03$, s.e.e. = 13.6. Right ventricular ^{201}Tl uptake was directly related to right ventricular wall thickness ($r = 0.56$, $p = 0.18$, s.e.e. = 10.4). Therefore, patients with more severe right ventricular systolic dysfunction have greater ^{201}Tl uptake after dipyridamole stress, suggesting increased myocardial mass and possibly blood flow in response to hypertrophy. Patients with the most marked hypertrophy have impairment of right ventricular systolic function, independent of ischemia.

J Nucl Med 1993; 34:1695–1700

In patients with pulmonary artery hypertension, development of right ventricular enlargement and dysfunction is associated with poor survival (*1–4*). Previous studies have documented the decline in right ventricular systolic function that occurs with pressure overload (*5–7*). Right ventricular systolic dysfunction also occurs in experimental preparations as pulmonary artery pressure is increased (*8,9*). Part of the decline in function in these models is related to ischemia. The right ventricle is susceptible to ischemia when pulmonary artery pressure is raised and coronary reserve becomes limited (*8–11*).

In patients with pulmonary hypertension, the hypertrophied right ventricle may be susceptible to ischemia. Thallium-201 is widely used to depict left ventricular myocardial blood flow. Since right ventricular mass (*12*) and blood flow/gram of myocardium (*13,14*) are substantially less than for the left ventricle, the former is usually only faintly seen on standard planar imaging in patients. One would expect increased uptake in patients with right ventricular hypertrophy. Few studies have described increased right ventricular ^{201}Tl uptake in patients with pulmonary artery hypertension (*15,16*). The purpose of this investigation was to analyze right ventricular ^{201}Tl uptake in patients with longstanding pulmonary artery hypertension to determine how ^{201}Tl kinetics relate to right ventricular size and function, and if these patients show evidence of right ventricular ischemia.

MATERIALS AND METHODS

Patients

Over a 3-mo period, we studied 19 patients with pulmonary artery hypertension who were being considered for heart-lung transplantation. A dipyridamole ^{201}Tl perfusion scan was ordered as part of the transplant evaluation to exclude significant coronary artery disease. There were 9 men and 10 women, age 34 ± 7 yr. The primary diagnoses and duration of symptoms are listed in Table 1. Most patients were severely disabled and could not exercise. All xanthine preparations were withheld for at least 72 hr before testing. Other medications were not withheld prior to testing.

Dipyridamole Thallium-201 Scintigraphy

All patients received 300–400 mg of crushed oral dipyridamole dissolved in orange juice. The heart rate and cardiac rhythm were monitored continuously. The blood pressure and 12-lead ECG were obtained every 5 min. After 40 min, 2.5 mCi of ^{201}Tl was given intravenously. The patient had planar imaging using a conventional gamma camera (GE Starcam, Milwaukee, WI) and a general all-purpose collimator. A symmetrical 20% window centered around the 68–80 keV mercury x-rays and a 10% window on

Received Feb. 23, 1993; revision accepted June 4, 1993.

For correspondence and reprints contact: Douglas S. Schulman, MD, Medical College of Pennsylvania, Allegheny General Hospital, 320 E. North Ave., Pittsburgh, PA 15212.

TABLE 1
Clinical Data

	Diagnosis	Duration (yr)	Age (yr)	NYHA (Class)	RVH	PAS (mmHg)	RVEF (%)
Group 1							
1	Cobalt	17	52	4	0	54	24
2	PPH	4	32	4	+	90	10
3	Sarcoid	8	39	4	+	60	26
4	PA Stenosis	31	31	3	+	120	28
5	PPH	5	42	3	+	87	29
6	MCTD	5	26	3	+	81*	16
7	Alpha-1	15	34	2	+	55*	24
8	PPH	5	43	3	+	90	27
9	PPH	4	37	4	+	100	10
M		10	37	3.3		82	22
s.d.		9	8	0.7		22	8
Group 2							
10	VSD	3	19	2	+	140	54
11	Eos Gran	8	39	2	+	64*	35
12	VSD	28	38	2	+	94	59
13	PDA	4	33	3	+	140	36
14	CF	12	27	4	+	71*	66
15	PPH	4	29	3	+	86	43
16	CF	4	28	2	+	81*	39
17	Bronch	8	33	3	0	46	38
18	CF	7	31	3	+	42	37
19	PPH	3	30	3	+	88	44
M		8	31	2.7		85	45
s.d.		7	6	0.7		34	11

*Pressure estimated by doppler echocardiography.

Alpha-1 = alpha-1 antitrypsin deficiency; Bronch = bronchiectesis; Cobalt = cobalt lung disease; CF = cystic fibrosis; Eos Gran = eosinophilic granuloma; M = mean; MCTD = mixed connective tissue disease; NYHA = New York Heart Association; PA = pulmonary artery; PAS = pulmonary artery systolic pressure; PDA = patent ductus arteriosus; PPH = primary pulmonary hypertension; s.d. = standard deviation; RVEF = right ventricular ejection fraction; RVH = right ventricular hypertrophy by ECG; VSD = ventricular septal defect.

the 167 keV peak were used. The initial set of images was obtained approximately 5 min after ^{201}Tl injection. Images were obtained for a preset time of 8 min. All images were stored on a computer disc in a 128 × 128 matrix format for later processing. The first image was obtained in the view that gave best septal separation. The camera was then rotated 30 degrees RAO and then 30 degrees LAO from the best septal view. A fourth image was obtained by lying the patient on his right side in the true lateral position. After the initial set of images were acquired, all patients received 100 mg of intravenous aminophylline. A second set of images was obtained 4 hr after the initial images in the same positions.

Qualitative Thallium-201 Analysis

The perfusion scans were interpreted subjectively without knowledge of clinical data. The images were graded for the concentration of ^{201}Tl in the region of the right ventricular free wall on the best LAO image. Right ventricular activity was graded as 3+ for activity greater than that in the left ventricular free wall, 2+ for activity equal to that of the left ventricular free wall and 1+ for activity less than that in the left ventricular free wall. The size of the right ventricular cavity was compared qualitatively to that of the left. The right ventricle was considered dilated if its cavity was greater than the left ventricle.

Quantitative Thallium-201 Analysis

Quantitative analysis of both ventricles was performed. The processing involved modified bilinear interpolative background subtraction and standard 9-point smoothing according to previously described techniques (*17–19*). In order to separate the ventricles, analysis of the best LAO image was performed. A region of interest (ROI) was drawn over the lateral wall of the left ventricle on the background subtracted image and the counts/pixel recorded. The computer positioned the identical region over this area on the delayed image. The percent washout represents the difference in counts/pixel of the left ventricular lateral wall between the initial and delayed image, normalized for the initial counts (*18,19*). A similar analysis was performed for the right ventricle. In the best LAO view, a ROI was drawn on the background subtracted image over the right ventricular free wall. The septum was not included in the region. The computer positioned the same ROI over the right ventricle in the delayed images and the percent washout was computed from the percent change in counts/pixel between the two ROIs. The ratio of right-to-left ventricular uptake was computed by comparing counts/pixel in the respective ROIs on the stress view.

Right Ventricular Ejection Fraction

After ^{201}Tl imaging, the patients' red blood cells were labeled in vivo with 25 mCi of ^{99m}Tc. A gamma camera (GE Starcam or Picker) equipped with a low-energy, all-purpose parallel-hole collimator was positioned in the LAO position which gave best septal separation with 10–15 degrees of caudal tilt. Gated equilibrium radionuclide angiograms were obtained in a 32-frame per cardiac cycle format. The gated studies were analyzed using a semi-automatic program which generated ROIs over the right ventricle in systole and diastole. The frames were displayed in an endless loop movie format to assist in edge detection. A phase image was generated to aid in separation of the right atrium and ventricle. From the ROIs, a background corrected time activity curve was generated from which right ventricular ejection fraction was calculated (*20*).

Echocardiography

Standard two-dimensional echocardiography was performed. Adequate data for interpretation of right ventricular size and wall thickness were available in 17 patients. Right ventricular wall thickness was measured in the subcostal view. The transverse diameter of the right ventricular outflow tract was measured in the short axis view at the level of the mitral valve. The diameter of the right ventricular inflow tract was measured in the apical four chamber view at the tricuspid valve level.

Hemodynamics

Most patients (n = 14) had right heart catheterization performed within 3 mo of the noninvasive evaluation. The catheterization was performed with a standard Swan-Ganz catheter. In the remaining five patients, pulmonary artery systolic pressure was estimated from Doppler echocardiographic recording of the velocity of the regurgitant jet of the tricuspid valve according to previously published methods (*21*).

Analysis

Data are presented as mean ± s.d. Differences between Groups 1 and 2 (see below) were compared by Student's t-test for unpaired data. Linear regression analysis was performed between right ventricular wall thickness, size, ejection fraction and pressures, and right ventricular free wall ^{201}Tl uptake.

RESULTS

Clinical Data

The patients had symptoms for an average of 9.2 ± 8 yr. In 14 patients, symptoms were NYHA Class III or IV. The remaining five patients had Class II symptoms. All but two patients had right ventricular hypertrophy on their 12-lead ECG (*22*). Home oxygen was required by 11 patients. The majority required treatment with digoxin, diuretics and calcium channel blockers. All patients had elevated pulmonary artery pressures (mean pulmonary artery systolic pressure 84 ± 28 mmHg).

Response to Dipyridamole

At 40 min after dipyridamole ingestion, the patients had a mild but significant decline from baseline in supine systolic blood pressure (125 ± 10 to 113 ± 12 mmHg, $p < 0.002$) with no change in diastolic pressure. The heart rate increased (88 ± 9 to 97 ± 7, $p < 0.001$). No patient developed chest pain or significant ST segment depression during monitoring. Gastrointestinal tract side effects were common (Table 1).

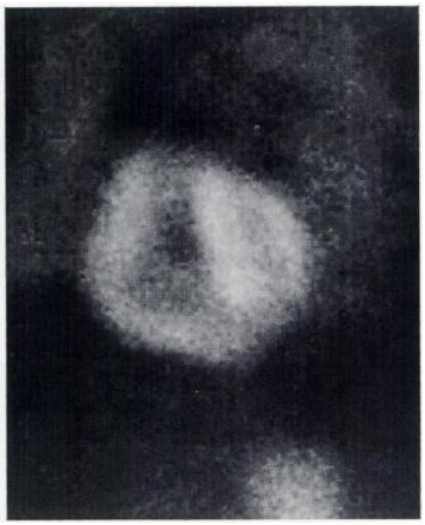

FIGURE 1.
Example of a best LAO view after dipyridamole vasodilation in a Group 1 patient. Note marked right ventricular ^{201}Tl uptake, chamber dilatation and small left ventricle.

Ventricular Function

The mean right ventricular ejection fraction was 34% ± 15% (range 10%–66%). In our laboratory, we consider severe right ventricular dysfunction as an ejection fraction <30%. We dichotomized the patients into two groups on this basis. There were nine patients who had severe dysfunction with a right ventricular ejection fraction <30% (mean 22% ± 8%, Group 1). The remaining 10 patients with ejection fractions >30% had a mean right ventricular ejection fraction of 45% ± 11%, (Group 2). Although disease duration and mean NYHA Class tended to be greater in Group 1 versus Group 2, pulmonary artery systolic pressure was similar in the two groups. Right ventricular wall thickness tended to be greater in Group 1 compared to Group 2 (1.4 ± 0.14 versus 0.95 ± 0.03 cm, $p = 0.13$). Right ventricular outflow tract dimension was 3.72 ± 0.40 cm in Group 1 versus 3.25 ± 0.47 cm in Group 2, $p < 0.05$. Right ventricular inflow tract dimension also tended to be greater in Group 1 versus Group 2 (5.43 ± 1.01 versus 4.56 ± 0.69 cm, $p = 0.07$). Left ventricular ejection fraction was normal in all patients. No patient had left ventricular hypertrophy on the ECG or two-dimensional echocardiogram.

Qualitative Thallium-201

No patient had a left or right ventricular perfusion abnormality on the planar images (Fig. 1). In Group 1, three of nine patients had 3+ right ventricular ^{201}Tl uptake. The remaining six patients had 2+ uptake. In Group 2, three of ten patients had 3+, two patients had 2+ and five patients had 1+ uptake. The mean uptake score was 2.4 ± 0.5 in Group 1 versus 1.8 ± 0.9 in Group 2, $p < 0.08$. In Group 1, seven patients had right ventricular dilatation versus three Group 2 patients (Chi Square = 2.63, $p = 0.1$).

Quantitative Thallium-201

In Group 1, counts/pixel in the right ventricular lateral wall on the stress view were increased compared to Group 2 (40 ± 7 versus 28 ± 15 counts/pixel, $p < 0.05$). Left ventricular free wall ^{201}Tl uptake on the dipyridamole

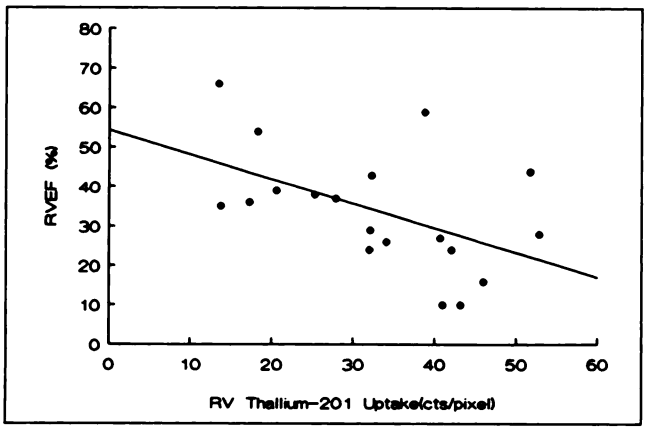

FIGURE 2. Relation between right ventricular ejection fraction (RVEF) and initial right ventricular (RV) ^{201}Tl uptake.

stress image was similar in both groups (51 ± 14 versus 54 ± 21 counts/pixel). Therefore, the ratio of right-to-left ventricular ^{201}Tl uptake during pharmacologic vasodilatation was greater in Group 1 versus Group 2 (0.81 ± 0.30 versus 0.49 ± 0.18, $p < 0.05$). Right ventricular free wall ^{201}Tl washout was comparable between the two groups; 51% ± 13% versus 51% ± 18% in Groups 1 and 2, respectively. Left ventricular free wall washout was also similar between Groups 1 and 2 (49% ± 15% versus 53% ± 13%). Right ventricular ejection fraction was inversely related to initial right ventricular ^{201}Tl uptake ($r = -0.49$, $p < 0.03$, s.e.e. = 13.6 (Fig. 2)) to right ventricular wall thickness ($r = -0.47$, $p = 0.05$, s.e.e. = 14.6) and to right ventricular dimension ($r = -0.50$, $p = 0.04$, s.e.e. = 14.3). Initial right ventricular ^{201}Tl uptake was also related to ventricular size. Initial right ventricular free wall ^{201}Tl uptake was directly related to right ventricular wall thickness ($r = 0.56$, $p = 0.18$, s.e.e. = 10.4) and inflow tract dimension ($r = 0.58$, $p = 0.15$, s.e.e. = 10.3). There was no relation between right ventricular ^{201}Tl uptake and systolic pulmonary artery pressure ($n = 19$) or right atrial pressure ($n = 14$). Right ventricular ^{201}Tl uptake tended to be related to the calculated pulmonary vascular resistance ($n = 14$) ($r = 0.46$, $p < 0.1$, s.e.e. = 11.6).

DISCUSSION

The response of the right ventricle to increased afterload is to dilate and hypertrophy. Horan and colleagues showed a linear relation between right ventricular mass and free wall area in 1500 human hearts at autopsy (*23*). By dilating, the right ventricle uses the Frank-Starling mechanism, increasing its preload to maintain cardiac output (*24,25*). Hypertrophy allows normalization of wall stress and improved ejection performance (*26*), yet, prolonged overload impairs contractility (*27*). Eventually, the right ventricle fails and cor pulmonale occurs. In patients with pulmonary artery hypertension, the development of cor pulmonale is a poor prognostic sign and a major cause of death (*1–4*). Whether right ventricular ischemia contributes to the systolic dysfunction was explored by analyzing ^{201}Tl kinetics in this setting.

Despite the excessive and prolonged afterload, results fail to substantiate the presence of myocardial ischemia as a major factor contributing to right ventricular dysfunction. In experimental preparations, elevations in pulmonary artery pressure cause a decline in right coronary artery vascular reserve and ischemia (*8,11*). Likewise, in systemic hypertension, coronary vascular reserve can be impaired and is related to ^{201}Tl perfusion abnormalities (*28*). However, in our patients with significant pulmonary hypertension, we failed to demonstrate either right ventricular perfusion defects or abnormal ^{201}Tl kinetics to suggest ischemia. Differences between right and left ventricular pressure overload may be related to the known variations in coronary flow patterns between the two ventricles (*29*). In addition, since patients with systemic hypertension and normal left ventricular mass have abnormal coronary flow reserve, systemic hypertension may be related to small vessel pathology and abnormal coronary vasodilator response independent of left ventricular hypertrophy (*30*). A similar primary small vessel abnormality may not exist in the right ventricles of patients with pulmonary hypertension. We cannot exclude the possibility that subendocardial ischemia was occurring and was in part responsible for the systolic dysfunction. Additional studies evaluating right ventricular ^{201}Tl kinetics at several points in time after injection, and right ventricular flow and metabolism with positron emission tomography, may help determine the potential role of ischemia in this setting.

Since initial ^{201}Tl uptake is proportional to myocardial blood flow (*31–33*), it is likely that our Group 1 patients had increased right coronary flow after vasodilatation compared to patients in Group 2. Flow may have been increased in response to right ventricular enlargement (*34*). Since these patients had more right ventricular dilatation on two-dimensional echocardiography and on planar imaging, greater right ventricular wall thickness, and more prolonged illness, it may be that they had a greater duration of right ventricular overload leading to systolic dysfunction. The direct relationships between right ventricular wall thickness and size and dipyridamole stress ^{201}Tl uptake confirm that patients with the greatest right ventricular mass have more prominent ^{201}Tl uptake. The inverse relationship between initial ^{201}Tl uptake and ejection fraction suggests that these patients with the greatest hypertrophy have worse ventricular function. This implication is confirmed by the inverse relationship between both right ventricular wall thickness and dimension and right ventricular ejection fraction. In a similar fashion, decreased left ventricular contractility has been reported in prolonged left ventricular pressure overload in patients with aortic stenosis (*35,36*) and systemic hypertension (*37*).

There are few studies which have analyzed right ventricular ^{201}Tl uptake. Cohen et al. first showed that right ventricular ^{201}Tl uptake is increased in patients with pulmonary artery hypertension (*15*). In a study of 99 patients with

a variety of cardiac diseases, Kondo et al. showed that right ventricular ^{201}Tl uptake increased linearly with right ventricular systolic and end-diastolic pressures and stroke-work (*16*). In an animal model of right ventricular hypertrophy, Rabinovitch et al. confirmed that right ventricular ^{201}Tl uptake correlated with mass and was increased significantly in animals with pulmonary artery hypertension compared to controls (*34*). Our results confirm these experimental reports showing significant correlations between right ventricular ^{201}Tl uptake and mass as estimated by dimension and wall thickness. We did not find a relationship between ^{201}Tl uptake and pulmonary artery or right atrial pressures. It may be that some of our patients with severe right ventricular overload had decreased pulmonary artery pressures due to lower cardiac output. The modest correlation between ^{201}Tl uptake and pulmonary vascular resistance supports this supposition.

Right ventricular ^{201}Tl kinetics have not been reported previously. Our washout rates for both ventricles at 4 hr were rapid and equivalent. Since washout rates are proportional to initial ^{201}Tl uptake (*38*), the near equal rates between the ventricles depict the marked right ventricular uptake in these patients. In patient studies, the myocardial clearance rate of ^{201}Tl appears to be slower after dipyridamole than exercise (*39,40*). The splanchnic bed acts as a reservoir, releasing the isotope into the blood causing higher blood levels and decreased gradient for myocardial washout (*40*). Our high levels of clearance may be related to differences in splanchnic uptake in patients with marked elevations in right heart pressures compared to normals.

Methodologic Issues

We used the right and left ventricular lateral walls on the view with best ventricular separation to quantitate ^{201}Tl uptake and washout. On this view, the two lateral walls are easily separated from the interventricular septum. We used oral dipyridamole to cause coronary vasodilatation. Intravenous dipyridamole was not available to us at the time of the study. Although oral dipyridamole may not be as reliable as the intravenous form, blood dipyridamole levels and effects appear to be similar when it is given intravenously (*41*). All our patients had a significant hemodynamic effect at the time of ^{201}Tl injection.

Changes in background (*42*) and other technical factors (*43*) can influence quantification of myocardial ^{201}Tl activity. High levels of splanchnic uptake can cause over-subtraction of myocardial counts (*44*). Nonetheless, one would not expect a difference in background subtraction in the patient groups. In addition, each patient acted as his own control since right ventricular uptake was normalized to left ventricular uptake. It is unlikely that differences in background subtraction, positioning or attenuation can explain the dissimilarity in ^{201}Tl uptake between the groups. Finally, the separation of our patients into two groups was arbitrary and based on our previous clinical segration of patients with right ventricular dysfunction. The linear relations between ^{201}Tl uptake, right ventricular ejection fraction and wall thickness suggest that these factors vary in a continuous manner.

In conclusion, patients with pulmonary hypertension have increased right ventricular ^{201}Tl uptake directly related to right ventricular size and inversely related to right ventricular systolic function.

REFERENCES

1. Fishman A. Pulmonary hypertension and cor pulmonale. In: Fishman A, ed. *Pulmonary diseases and disorders, second edition*. New York: McGraw-Hill, 1988:999–1048.
2. Hughes J, Rubin L. Primary pulmonary hypertension. An analysis of 28 cases and a review of the literature. *Medicine* 1986;65:56–72.
3. Wallcott G, Burchell HB, Brown AL Jr. Primary pulmonary hypertension. *Am J Med* 1970;49:70–81.
4. Traver G, Cline M, Burrows B. Predictors of mortality in chronic obstructive pulmonary disease. *Am Rev Respir Dis* 1979;119:895–902.
5. Brent BN, Mahler D, Matthay RA, Berger HJ, Zaret BL. Noninvasive diagnosis of pulmonary arterial hypertension in chronic obstructive pulmonary disease: right ventricular ejection fraction at rest. *Am J Cardiol* 1984; 53:1349–1353.
6. Korr KS, Gandsman EJ, Winkler ML, Shulman RS, Bough EW. Hemodynamic correlates of right ventricular ejection fraction measured with gated radionuclide angiography. *Am J Cardiol* 1982;49:71–77.
7. Konstam MA, Salem DN, Isner JM, et al. Vasodilator effect on right ventricular function in congestive heart failure and pulmonary hypertension: end-systolic pressure-volume relation. *Am J Cardiol* 1984;54:132–136.
8. Brooks H, Kirk ES, Vokonas PS, Urschel CW, Sonnenblick EH. Performance of the right ventricle under stress: relation to right coronary flow. *J Clin Invest* 1971;50:2176–2183.
9. Vlahakes GJ, Turley K, Hoffman JIE. The pathophysiology of failure in acute right ventricular hypertension: hemodynamic and biochemical correlations. *Circulation* 1981;63:87–95.
10. Gold FL, Bache RJ. Transmural right ventricular blood flow during acute pulmonary hypertension in the sedated dog. *Circ Res* 1982;51:196–204.
11. Manohar M, Tranquilli WJ, Parks CM, Benson J, Theodorakis MC, Thurmon JC. Regional myocardial blood flow and coronary vasodilator reserve during acute right ventricular failure due to pressure overload in swine. *J Surg Res* 1981;31:382–391.
12. Murray PA, Vatner SF. Fractional contributions of the right and left coronary arteries to perfusion of normal and hypertrophied right ventricles of conscious dogs. *Circ Res* 1980;47:190–200.
13. Yonekura S, Watanabe N, Caffrey JL, Gaugl JF, Downey HF. Mechanism of attenuated pressure-flow autoregulation in right coronary circulation of dogs. *Circ Res* 1987;60:133–141.
14. Fixler DE, Archie JP, Ullyot DJ, Buckberg GD, Hoffman JIE. Effects of acute right ventricular systolic hypertension on regional myocardial blood flow in anesthetized dogs. *Am Heart J* 1973;85:491–500.
15. Cohen HA, Baird MG, Rouleau JR, et al. Thallium-201 myocardial imaging in patients with pulmonary artery hypertension. *Circulation* 1976;54:790–795.
16. Kondo M, Kubo A, Yamazaki H, et al. Thallium-201 myocardial imaging for evaluation of right-ventricular overloading. *J Nucl Med* 1978;19:1197–1203.
17. Goris M, Daspit SG, McLaughlin P, Kriss JP. Interpolative background subtraction. *J Nucl Med* 1976;17:744–747.
18. Garcia E, Maddahi J, Berman C, Waxman A. Space/time quantitation of thallium-201 myocardial scintigraphy. *J Nucl Med* 1981;22:309–317.
19. Watson DD, Campbell NP, Read EK, Gibson RS, Teates CD, Beller GA. Spatial and temporal quantitation of plane thallium myocardial images. *J Nucl Med* 1981;22:577–584.
20. Maddahi J, Berman DS, Matsuoka DT. A new technique for assessing right ventricular ejection fraction using rapid multiple-gated equilibrium cardiac blood pool scintigraphy. Description, validation, and findings in chronic coronary artery disease. *Circulation* 1979;60:581–589.
21. Yock PG, Popp RL. Noninvasive estimation of right ventricular systolic pressure by doppler ultrasound in patients with tricuspid regurgitation. *Circulation* 1984;70:657–662.
22. Milnor WR. Electrocardiogram and vectorcardiogram in right ventricular hypertrophy and right bundle branch block. *Circulation* 1957;16:348–353.
23. Horan LG, Flowers NC, Havelda CJ. Relation between right ventricular mass and cavity size: an analysis of 1500 human hearts. *Circulation* 1981; 64:135–138.

24. Sibbald W, Drieger A. Right ventricular function in acute disease states: Pathophysiologic considerations. *Crit Care Med* 1983;11:339–345.
25. Weber K, Janicki J, Shroff S, et al. Contractile mechanics and interaction of the right and left ventricles. *Am J Cardiol* 1981;47:686–695.
26. Belik J, Light R. Effect of increased afterload on right ventricular function in newborn pigs. *J Appl Physiol* 1989;66:863–869.
27. Spann JF, Jr, Covell JW, Eckberg DL, Sonnenblick EH, Ross J, Jr, Braunwald E. Contractile performance of the hypertrophied and chronically failing cat ventricle. *Am J Physiol* 1972;223:1150–1157.
28. Matthay RA, Berger H, Davies R, et al. Right and left ventricular exercise performance in chronic obstructive pulmonary disease: radionuclide assessment. *Ann Intern Med* 1980;93:234–239.
29. Houghton JL, Frank MJ, Carr AA, von Dohlen, TW, Prisant M. Relations among impaired coronary flow reserve, left ventricular hypertrophy and thallium perfusion defects in hypertensive patients without obstructive coronary artery disease. *J Am Coll Cardiol* 1990;15:43–51.
30. Brush JE, Cannon RO, Schenke WH, et al. Angina due to coronary microvascular disease in hypertensive patients without left ventricular hypertrophy. *N Engl J Med* 1988;319:1302–1307.
31. Melin JA, Becker LC. Quantitative relationship between global left ventricular thallium uptake and blood flow: effects of propranolol, quabain, dipyridamole, and coronary artery occlusion. *J Nucl Med* 1986;27:641–652.
32. Nishiyama H, Adolph RJ, Gabel M, Lukes SJ, Franklin D, Williams CC. Effect of coronary blood flow on thallium-201 uptake and washout. *Circulation* 1982;65:534–542.
33. Strauss HW, Harrison K, Langan JK, Lebowitz E, Pitt B. Thallium-201 for myocardial imaging. *Circulation* 1975;51:641–645.
34. Rabinovitch M, Fisher K, Gamble W, Reid L, Treves S. Thallium-201: quantitation of right ventricular hypertrophy in chronically hypoxic rats. *Radiology* 1979;130:223–225.
35. Huber D, Grimm J, Koch R, Krayenbuehl HP. Determinants of ejection performance in aortic stenosis. *Circulation* 1981;64:126–134.
36. Wisenbaugh T, Booth D, DeMaria A, Nissen S, Waters J. Relationship of contractile state to ejection performance in patients with chronic aortic valve disease. *Circulation* 1986;73:47–53.
37. Tarazi RC, Levy M. Cardiac responses to increased afterload. State of the art review. *Hypertension* 1982;4(Suppl II):II-8–II-18.
38. Okada RD, Leppo JA, Boucher CA, Pohost GM. Myocardial kinetics of thallium-201 after dipyridamole infusion in normal canine myocardium and in myocardium distal to a stenosis. *J Clin Invest* 1982;69:199–209.
39. Varna SK, Watson DD, Beller GA. Quantitative comparison of thallium-201 scintigraphy after exercise and dipyridamole in coronary artery disease. *Am J Cardiol* 1989;64:871–877.
40. Ruddy TD, Gill JB, Finkelstein DM, et al. Myocardial uptake and clearance of thallium-201 in normal subjects: comparison of dipyridamole-induced hyperemia with exercise stress. *J Am Coll Cardiol* 1987;10:547–556.
41. Gould KL, Sorenson SG, Albro P, Caldwell JH, Chaudhuri T, Hamilton GW. Thallium-201 myocardial imaging during coronary vasodilation induced by oral dipyridamole. *J Nucl Med* 1986;27:31–36.
42. Steingart RM, Bontemps R, Scheuer J, Yipintsoi T. Gamma camera quantitation of thallium-201 redistribution at rest in a dog model. *Circulation* 1982;65:542–550.
43. Lancaster JL, Starling MR, Kopp DT, Lasher JC, Blumhardt R. Effect of errors in reangulation on planar and tomographic thallium-201 washout profile curves. *J Nucl Med* 1985;26:1445–1455.
44. Narahara KA, Hamilton GW, Williams DL, Gould KL. Myocardial imaging with thallium-201: an experimental model for analysis of the true myocardial and background image components. *J Nucl Med* 1977;18:781–786.